

X-Band Atmospheric Noise Temperature Statistics at Goldstone, DSS 13, 1979 and 1980, and Clear Air Noise Temperature Models for Goldstone

S. D. Slobin, C. T. Stelzried, E. M. Andres, and M. M. Franco
Radio Frequency and Microwave Subsystems Section

X-band noise temperature data have been taken at Goldstone DSS 13 continuously since August 1975. This article updates the statistics of noise temperature increase above quiescent baseline for the years 1979 and 1980. The X-band data base now consists of five complete years of measurements. This article also gives clear air models for Goldstone, showing the seasonal noise temperature effects of changing surface water vapor densities for a particular atmospheric model.

I. X-Band Atmospheric Noise Temperature Statistics at Goldstone, DSS 13, 1979 and 1980

A. Introduction

Previous DSN Progress Reports (Refs. 1-3) have presented descriptions of the Goldstone DSS 13 X-band radiometer used for the microwave weather project. Statistics of zenith noise temperature increase above quiescent baseline for the years 1975-1978 have also been presented. 1977 was a very dry year and 1978 was a very wet year. Cumulative distributions of noise-temperature increase for these two years tend to bracket the data for all the years. Comparisons with the existing CCIR (International Radio Consultative Committee) arid region global rain model (Ref. 4) and the cloud-based theoretical model of the DSN Flight Project Interface Design Handbook show the actual Goldstone measurements to lie between the two. This indicates that the existing models should be used and interpreted with caution for mission planning purposes.

The noise temperature increases described are due to the atmosphere alone and do not include the effects of ground and waveguide contribution. Included in the noise temperature data, however, are small *decreases* in cosmic background contribution due to increases in the atmospheric attenuation. This effect is quite small compared to actual atmospheric changes.

B. Noise Temperature Statistics

The cumulative distributions of noise temperature increase above quiescent baseline are shown in Fig. 1 for the years 1975 through 1980. As an example, for the year 1980, 90 percent of the time the zenith atmospheric noise temperature increase above the quiescent (undisturbed) baseline is 1 kelvin or less; 98 percent of the time the increase is 3 kelvins or less. Because of radiometer bias errors during the year, the 1980 curve is the result of adjusting the noise temperature values 0.5 kelvins higher; i.e., the initial data reduction yielded 0.5 kelvins at the 90 percent level; the adjusted value is 1.0 kelvins at the same percentage level. Table 1 shows cumulative distribu-

tions by year-quarter for 1979. Table 2 shows 1980 data biased such that only 10 percent of the values for each year-quarter lie below 0 kelvins increase. A negative increase is statistically valid because it includes the effects of radiometer jitter above and below a nominal value.

The change in zenith atmospheric attenuation associated with any noise temperature change may be calculated from the following expression:

$$\Delta A(\text{dB})_z = 10 \log_{10} \left[\frac{T_p}{T_p - \Delta T 10^{A_0/10}} \right]$$

where

T_p = effective physical temperature of the atmosphere,
 $\cong 280$ K

ΔT = noise temperature increase above baseline, kelvins

A_0 = baseline atmospheric attenuation at zenith,
 ≈ 0.036 dB at X-band at DSS 14

The atmospheric attenuation change at an elevation angle other than zenith may be approximated by:

$$\Delta A(\text{dB})_\theta = \frac{\Delta A(\text{dB})_z}{\sin \theta}$$

where

$\Delta A(\text{dB})_z$ = attenuation change at zenith

θ = nonzenith elevation angle

The noise temperature change at the nonzenith elevation angle may be calculated from:

$$\Delta T_\theta = T_p \left[1 - \frac{1}{10^{\Delta A_\theta/10}} \right] \cdot 10^{-A_0/10}$$

where all quantities are defined above.

II. Clear Air Noise Temperature Models for Goldstone

A. Effects of Various Surface Water Vapor Densities

The equation of radiative transfer has been integrated (for a particular atmospheric model) to determine microwave noise

temperature as a function of surface water vapor density and elevation angle for various commonly used microwave frequencies. Since water vapor is the most commonly changing component of the troposphere, its temporal variation will introduce uncertainties in what is normally referred to as the "clear sky" baseline. These variations in noise temperature may be rather large, particularly at frequencies near the "water vapor line" (22.235 GHz). Tables 3 and 4 present noise temperature and attenuation values for two antenna locations, sea level (as a reference) and a ground level of 1.032 km, the altitude of DSS 14 at Goldstone. For comparison, the altitudes of the other 64-meter antennas are 0.670 km (DSS 43, Canberra) and 0.796 km (DSS 63, Madrid).

The primary effect of changing altitude in these models is to alter the amount of oxygen through which the antenna looks. The water vapor contributions will remain substantially the same, subject only to the line-width pressure broadening effect of the total atmospheric pressure.

The particular atmospheric model used in these calculations is:

- (1) Water vapor density profile: $\rho = \rho_0 e^{-h/2.0}$

where

ρ_0 = surface water vapor density

h = height above surface, km

- (2) Temperature profile: 20°C at surface, -6.3 K/km lapse rate, 220 K minimum temperature

- (3) Sea level pressure 1013.6 mb, pressure profile

$$P = P_0 e^{-0.116 h},$$

h in km, pressure scale height = 8.62 km

The water vapor and oxygen absorption coefficients are calculated from expressions in Bean and Dutton (Ref. 5) modified slightly to yield agreement with values calculated by the J. W. Waters radiative transfer program (Ref. 6).

B. Seasonal Clear Air X- and K_A-Band Noise Temperature Models for Goldstone DSS 13

Using figures for yearly water vapor distribution in Bean and Dutton (Ref. 5), clear air (oxygen and water vapor) models for noise temperature may be developed for Goldstone DSS 13. The results for DSS 14 will be very similar since both stations are at nearly equal heights above sea level (DSS 13 = 1.094 km, DSS 14 = 1.032 km). Surface absolute humidity

(AH) amounts at Goldstone for “dry” and “wet” months are given in Table 5.

Assuming a normal (Gaussian) distribution of absolute humidity (not strictly true, however), 98% of the time (99% - 1%) the absolute humidity will lie within 2.33 standard deviations (2.33σ) of its mean value. Thus, for February, $1\sigma = ((9-2)/4.66) = 1.5 \text{ g/m}^3$. For August, $1\sigma = ((14-5)/4.66) = 1.9 \text{ g/m}^3$

Table 6 gives the water vapor seasonal *surface* models for the Goldstone area.

Based on previously calculated DSS 13 (very similar to DSS 14) models of oxygen and water vapor effects (using the model described above), the effects of these atmospheric components are given in Table 7.

Using Tables 6 and 7, the seasonal water vapor and oxygen noise temperature effects (mean $\pm 1\sigma$) can be calculated (Table 8). The mean is just the average of all year-quarters

(two quarters each being the mean of the wet and dry quarters). The yearly standard deviation (σ) of the sum of four normal seasonal distributions of different means and standard deviations is found from

$$\sigma^2 = \frac{1}{4} \sum_{i=1}^4 (\sigma_i^2 + \mu_i^2) - \mu^2$$

where

σ_i = standard deviation of each seasonal distribution

μ_i = mean of each seasonal distribution

μ = yearly mean

The numbers in parentheses in Table 8 are the $\pm 1\sigma$ spread. For a normal distribution (which the four seasons are postulated to have, but not the year), approximately 68% of the time the values will lie between $\pm 1\sigma$.

References

1. Reid, M. S., et al., “An X-Band Radiometer for the Microwave Weather Project,” in *The Deep Space Network Progress Report 42-29*, Jet Propulsion Laboratory, Pasadena, Calif., Feb. 15, 1975, pp. 54-59.
2. Slobin, S. D., et al., “X-Band Atmospheric Noise Temperature Statistics at Goldstone DSS 13, 1975-1976,” in *The Deep Space Network Progress Report 42-38*, Jet Propulsion Laboratory, Pasadena, Calif., Apr. 15, 1977, pp. 70-76.
3. Slobin, S. D., et al., “X-Band Atmospheric Noise Temperature Data and Statistics at Goldstone, DSS 13, 1977-1978,” in *The Deep Space Network Progress Report 42-52*, Jet Propulsion Laboratory, Pasadena, Calif., Aug. 15, 1979, pp. 108-116.
4. CCIR Study Group, WARC-79, Document P/105-E, “Rain Attenuation Prediction,” Geneva, Switzerland, 6 June 1978.
5. Bean, B. R., and Dutton, E. J., *Radio Meteorology*, Dover Publications, New York, 1968.
6. Smith, E. K., and Waters, J. W., “A Comparison of CCIR Values of Slant Path Attenuation and Sky Noise Temperature With Those From the JPL Radiative Transfer Program,” presented at URSI National Radio Science Meeting, Boulder, Colorado, January 12-16, 1981.

Table 1. Cumulative distributions of zenith atmospheric noise temperature increases above quiescent baseline at Goldstone, 1979

TZX ^a	1st year-quarter	2nd year-quarter	3rd year-quarter	4th year-quarter	Year total
0	0.081	0.203	0.234	0.281	0.182
1	0.880	0.983	0.983	0.890	0.936
2	0.916	0.995	0.991	0.938	0.960
3	0.930	0.998	0.993	0.964	0.970
4	0.941	0.999	0.994	0.986	0.977
5	0.948	0.999	0.995	0.995	0.980
6	0.955	0.999	0.995	0.996	0.983
7	0.960	0.999	0.995	0.997	0.985
8	0.964	0.999	0.995	0.997	0.986
9	0.968	0.999	0.996	0.997	0.988
10	0.971	0.999	0.996	0.997	0.989

^aTZX = X-band zenith atmospheric noise temperature increase above quiescent baseline, K; e.g., 1st year-quarter, TZX = 3, 93.0% of data below 3-K increase.

Table 2. Cumulative distributions of zenith atmospheric noise temperature increases above quiescent baseline at Goldstone, 1980 (with biases, see text)

TZX ^a	1st year-quarter	2nd year-quarter	3rd year-quarter	4th year-quarter	Year total
0	0.100	0.100	0.100	0.100	0.320
1	0.650	0.850	0.700	0.928	0.885
2	0.905	0.977	0.989	0.997	0.975
3	0.920	0.981	0.998	0.999	0.980
4	0.930	0.982	0.999	0.999	0.982
5	0.940	0.983	1.000	1.000	0.984
6	0.947	0.984	1.000	1.000	0.986
7	0.953	0.984	1.000	1.000	0.987
8	0.956	0.985	1.000	1.000	0.988
9	0.961	0.985	1.000	1.000	0.989
10	0.966	0.986	1.000	1.000	0.990

^aTZX = X-band zenith atmospheric noise temperature increase above quiescent baseline, K; e.g., 2nd year-quarter, TZX = 3, 98.1% of data below 3-K increase.

**Table 3. Clear air noise temperature and attenuation, 90° elevation angle
(W = surface water vapor density)**

Location and altitude	Atmosphere components $O_2 + W \text{ g/m}^3 \text{ WV}$	90° elevation							
		2.3 GHz		8.5 GHz		21.0 GHz		32.0 GHz	
		T, K	A, dB	T, K	A, dB	T, K	A, dB	T, K	A, dB
Sea level	$O_2 + 0.0 \text{ g/m}^3$	2.12	0.035	2.29	0.038	3.23	0.053	6.38	0.106
$H = 0.000 \text{ km}$	$O_2 + 3.0 \text{ g/m}^3$	2.13	0.035	2.48	0.041	10.30	0.163	9.54	0.154
	$O_2 + 7.5 \text{ g/m}^3$	2.15	0.035	2.78	0.045	20.50	0.327	14.29	0.228
	$O_2 + 10.0 \text{ g/m}^3$	2.16	0.036	2.94	0.048	25.98	0.417	16.94	0.270
	$O_2 + 15.0 \text{ g/m}^3$	2.18	0.036	3.28	0.053	36.52	0.597	22.24	0.355
DSS 14	$O_2 + 0.0 \text{ g/m}^3$	1.68	0.028	1.80	0.030	2.54	0.042	5.03	0.083
$H = 1.032 \text{ km}$	$O_2 + 3.0 \text{ g/m}^3$	1.69	0.028	1.98	0.032	9.95	0.157	7.87	0.127
	$O_2 + 7.5 \text{ g/m}^3$	1.70	0.028	2.24	0.036	20.65	0.328	12.14	0.193
	$O_2 + 10.0 \text{ g/m}^3$	1.71	0.028	2.39	0.038	26.37	0.423	14.52	0.230
	$O_2 + 15.0 \text{ g/m}^3$	1.73	0.029	2.69	0.043	37.40	0.611	19.30	0.306

**Table 4. Clear air noise temperature and attenuation, 30° elevation angle
(W = surface water vapor density)**

Location and altitude	Atmosphere components $O_2 + W \text{ g/m}^3 \text{ WV}$	30° elevation							
		2.3 GHz		8.5 GHz		21.0 GHz		32.0 GHz	
		T, K	A, dB	T, K	A, dB	T, K	A, dB	T, K	A, dB
Sea level	$O_2 + 0.0 \text{ g/m}^3$	4.21	0.070	4.56	0.075	6.41	0.106	12.61	0.212
$H = 0.000 \text{ km}$	$O_2 + 3.0 \text{ g/m}^3$	4.24	0.070	4.94	0.081	20.22	0.326	18.76	0.309
	$O_2 + 7.5 \text{ g/m}^3$	4.28	0.071	5.53	0.090	39.56	0.654	27.87	0.457
	$O_2 + 10.0 \text{ g/m}^3$	4.30	0.071	5.86	0.095	49.64	0.835	32.89	0.540
	$O_2 + 15.0 \text{ g/m}^3$	4.35	0.072	6.52	0.105	68.48	1.194	42.80	0.710
DSS 14	$O_2 + 0.0 \text{ g/m}^3$	3.34	0.055	3.60	0.059	5.06	0.084	9.98	0.167
$H = 1.032 \text{ km}$	$O_2 + 3.0 \text{ g/m}^3$	3.36	0.056	3.94	0.065	19.57	0.314	15.52	0.253
	$O_2 + 7.5 \text{ g/m}^3$	3.40	0.056	4.46	0.072	39.83	0.656	23.77	0.385
	$O_2 + 10.0 \text{ g/m}^3$	3.42	0.056	4.75	0.077	50.37	0.846	28.32	0.460
	$O_2 + 15.0 \text{ g/m}^3$	3.46	0.057	5.35	0.086	70.01	1.221	37.34	0.611

Table 5. Surface absolute humidity values for Goldstone area

Month	AH exceeded 99% of time	Mean	AH exceeded 1% of time
Feb. (dry)	2 g/m ³	5 g/m ³	9 g/m ³
Aug. (wet)	5 g/m ³	10 g/m ³	14 g/m ³

Table 6. Surface water vapor density for Goldstone area

Month	Surface water vapor density, g/m ³
February (dry)	AH = 5.0 ± 1.5 (1σ)
August (wet)	AH = 10.0 ± 1.9 (1σ)

Table 7. Noise temperature effects for oxygen and water vapor (DSS 13)

Component	X-band (8.5 GHz)		K _A -band (32 GHz)	
	90° elevation	30° elevation	90° elevation	30° elevation
Oxygen	1.78 K	3.54 K	4.96 K	9.84 K
Water vapor 1 g/m ³	0.058 K	0.12 K	0.94 K	1.82 K

Table 8. Seasonal clear-air noise temperature models for DSS 13, mean ± 1 std deviation

Elevation angle	Atmospheric noise temperature, K at X-band (8.5 GHz)			Atmospheric noise temperature, K at K _A -band (32 GHz)		
	Feb	Aug	Year	Feb	Aug	Year
90°	2.07 ± 0.09 (1.98 – 2.16)	2.36 ± 0.11 (2.25 – 2.47)	2.22 ± 0.10 (2.12 – 2.32)	9.68 ± 1.41 (8.27 – 11.09)	1439 ± 1.79 (12.60 – 16.18)	12.04 ± 2.30 (9.74 – 14.34)
30°	4.12 ± 0.17 (3.95 – 4.29)	4.69 ± 0.22 (4.47 – 4.91)	4.41 ± 0.24 (4.17 – 4.65)	18.94 ± 2.73 (16.21 – 21.67)	28.04 ± 3.46 (24.58 – 31.50)	23.49 ± 4.47 (19.02 – 27.96)

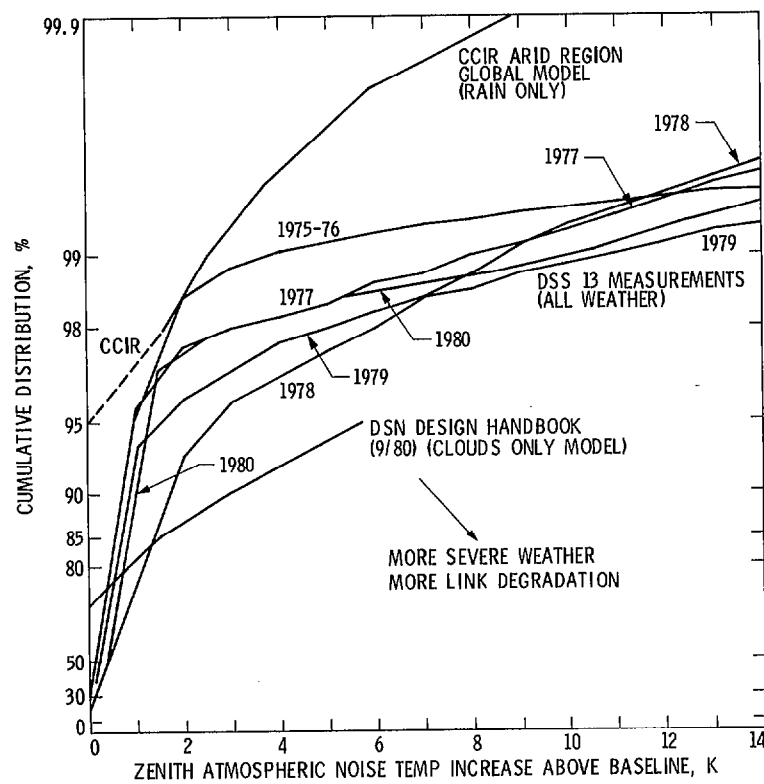


Fig. 1. Cumulative distributions of X-band zenith atmospheric noise temperature increase above quiescent baseline at Goldstone DSS 13